

Experimental Characterization of a Quadrotor's Response to an Air Vortex Cannon

Kyle VanHorn *

University of North Carolina at Charlotte, Charlotte, NC, 28223

Unmanned aerial vehicles (UAVs) play an important role in civilian and military operations. They are being used in a wide array of applications, from military reconnaissance to commercial deliveries. UAVs are particularly useful in hostile environments, as they are able to remove the operator from potentially dangerous situations. A threat to UAVs in such environments is their vulnerability to shockwaves and blasts. Directed energy systems are a proven method of destabilizing UAVs due to shockwaves. UAVs are highly sensitive to both impulsive pressure disturbances and mechanical vibrations, which affect sensors and overall stability. This paper investigates the response of a micro-quadrotor, the Crazyflie 2.1, exposed to a sudden aerodynamic force generated by a directed blast from a vortex cannon while in hovering flight. The vortex blasts were generated from varying distances to adjust the intensities experienced by the quadrotor. In addition, the relative impact angle of the vortex ring to the drone was varied. Onboard inertial measurement unit (IMU) data was recorded during each quadrotor-vortex interaction. The sensors analyzed included 3-axis gyroscope, 3-axis accelerometer, and barometer (temperature and pressure), as well as the drones estimated pitch, roll, and yaw. The drone was subjected to increasing intensity of blasts, until the drone was destabilized and unable to recover. Analysis of the flight data showed that the drone experienced a sudden change of pressure, on the order of 20 to 40 Pascals, a few tenths of a second prior to major perturbations as measured by the gyroscope and accelerometer. These findings indicate that the barometer detects a pressure change from the vortex prior to the drone destabilizing, allowing a window where preemptive flight maneuvers can be performed to be more resistant to the vortex. These findings offer new insights into UAV sensor fusion and control strategies under impulsive disturbances, paving the way for improved stability and survivability in high-threat environments.

Nomenclature

ΔP	=	change in pressure (derivative of pressure)
Bluetooth LE	=	Bluetooth Low Energy
cflib	=	Crazyflie Python Library
IMU	=	inertial measurement unit
ISM	=	Industrial, Scientific, and Medical
LPS	=	Loco Positioning System
MAV	=	micro aerial vehicle
MEMS	=	Micro-Electromechanical Systems
Std	=	standard deviation
TDoA	=	time delay of arrival
ToF	=	time of flight
TWR	=	two-way ranging
UAV	=	uncrewed aerial vehicle

*Undergraduate Researcher, Mechanical Engineering and Engineering Science, AIAA Student Member (1314973).

I. Introduction

UNCREWED aerial vehicles (UAV's) are becoming an integral part of modern technological advancements, with applications spanning across defense, search and rescue, healthcare, package delivery, agriculture, and environmental monitoring. Their ability to operate remotely makes them invaluable in scenarios where human presence is either impractical or hazardous. In particular, UAVs play a critical role in military and defense operations, where they are used for reconnaissance, surveillance, and tactical engagements. A key advantage of UAVs in these environments is their capacity to operate in hostile or high-risk zones while keeping human operators at a safe distance.

However, UAVs are highly dependent on onboard sensors to maintain stable flight. These sensors - such as gyroscopes, accelerometers, and barometers - provide essential data for flight control systems, ensuring that the aircraft can respond appropriately to environmental disturbances. In high-threat environments, such as combat zones, UAVs are susceptible to external forces that can interfere with their stability. Shockwaves from explosions, blasts, and directed energy weapons can introduce sudden pressure disturbances and mechanical vibrations that impact sensor readings, potentially leading to flight instability or complete loss of control.

Understanding the response of UAVs to such impulsive forces is essential for improving their resilience and survivability in dynamic environments. This study examines the effects of sudden aerodynamic impulses on a micro-quadrotor in a controlled laboratory setting. To simulate the effects of an explosive blast, an air vortex cannon is used to generate directed pressure waves toward the drone. The UAV's response is recorded using onboard inertial measurement unit (IMU) sensors, as well as through slow-motion video capture. The insights gained from this research contribute to the broader field of UAV control strategies, sensor fusion, and stability enhancement in high-threat environments.

II. Related Works

The vulnerability of UAVs to external disturbances, particularly shockwaves and blasts, has been the subject of several prior research studies. This section highlights relevant prior work that investigates the effects of directed energy, blast waves, and vibroacoustic interference on UAV stability and structural integrity. While these studies provide significant insights, our study distinguished itself by focusing on real-time onboard sensor responses to directed aerodynamic blasts and their implication for UAV flight control and stabilization.

Martin et al. from Sandia National Laboratories examined the vulnerability of UAVs to directed acoustic energy [1]. Their study focused on using high-intensity acoustic impulses to disrupt the inertial measurement unit of UAVs, causing destabilization. The researchers found that moderate-amplitude acoustic monotonics at specific resonant frequencies of MEMS gyros and accelerometers could severely affect UAV flight stability. This work demonstrated the feasibility of using non-destructive targeted acoustic energy as an anti-UAV countermeasure.

Feng et al. investigated the damage assessment methodology for UAVs subjected to blast waves [2]. Their research focused on fixed-wing UAVs, analyzing the structural response to blast loading using numerical simulations and experiments with explosive charges. They identified shear force as a key damage parameter, with complete wing failure occurring at a critical overpressure threshold. This study provided a framework for quantifying UAV structural damage due to explosive impacts.

Grywinski and Zygadlo explored vibroacoustic disturbances on UAVs [3]. Their research analyzed mechanical and aerodynamic sources of interference that affect UAV sensor accuracy, particularly in high-vibration environments. They found that engine-induced mechanical vibrations and periodic aerodynamic fluctuations create complex multi-modal disturbances, which can degrade sensor performance and measurement accuracy.

Gupta, Sane, and Arakeri developed a vortex ring generator to study gust impacts [4]. Their study presents a robust and highly controllable method for generating discrete aerodynamic gusts in a laboratory setting. By characterizing the vortex ring flow properties through both flow visualization and novel light bead method, they demonstrated that such a device can be used to simulate natural gusts affecting flying bodies. Although their experiments were conducted on freely flying soldier flies and focused on fluid-structure interaction at high Reynolds numbers, the methodology provides valuable insights for applying similar controlled gust-generation techniques to UAV research.

Zieg and Liu conducted an experimental study on the impact of blast waves on UAV aerodynamic properties [5]. Their research used a NACA0012 airfoil model to study supersonic fluid-structure interactions. By exposing the airfoil to a blast, they observed significant aerodynamic changes, demonstrating how shockwaves can alter lift and stability.

Tao and Zhang studied the vibration and wave propagation in ship-borne tethered UAVs using stress wave methods [6]. Their work established a dynamic model that incorporated geometric nonlinearity and equilibrium curvature effects to explain how standing waves and subharmonic components in tethered systems influence UAV stability.

While previous studies have examined UAV responses to directed energy, blast waves, and vibroacoustic disturbances, this work focuses on real-time sensor data captured during exposure to directed aerodynamic impulses generated by an air vortex cannon. Unlike Martin et al., who investigated acoustic energy effects on UAV IMUs, this research examines the response to aerodynamic shockwaves. In contrast to Feng et al., who assessed UAV structural damage under explosive blast loading, this study concentrates on flight stability and sensor-level pressure dynamics. This approach provides a new perspective on UAV recovery dynamics and preemptive control strategies in high-threat environments.

III. Hardware

A. Crazyflie 2.1 Micro-Aerial Vehicle

The drone employed in this work was the Crazyflie 2.1 platform, developed and manufactured by Bitcraze. The Crazyflie is a 27g, open source flying development platform specifically designed for education, research, and swarming. The Crazyflie uses a printed circuit board (PCB) as the frame of the drone [7]. A Crazyflie can be seen in Fig. 1.

The Crazyflie is equipped with both radio and Bluetooth Low Energy (LE). It can be controlled using a mobile device over Bluetooth or with a computer and the Bitcraze Crazyradio 2.0. The Crazyradio 2.0 is a USB radio dongle compatible with the Crazyflie ecosystem. It is based on the nRF52840 from Nordic Semiconductor and communicates with the Crazyflie over 2.4 GHz Industrial, Scientific, and Medical (ISM) band radio [8].

In this work, the Crazyflies were operated using a Crazyradio connected to a Windows computer. The Crazyflies were controlled autonomously using Python and the Crazyflie Python Library [9]. Python scripts were written to send commands to the Crazyflie.

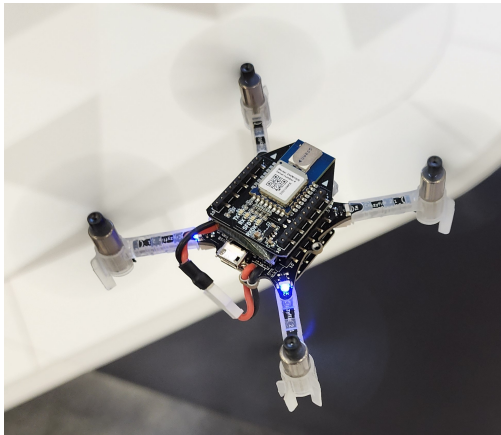


Fig. 1 Crazyflie 2.1 in Flight, Equipped with Loco Positioning Deck

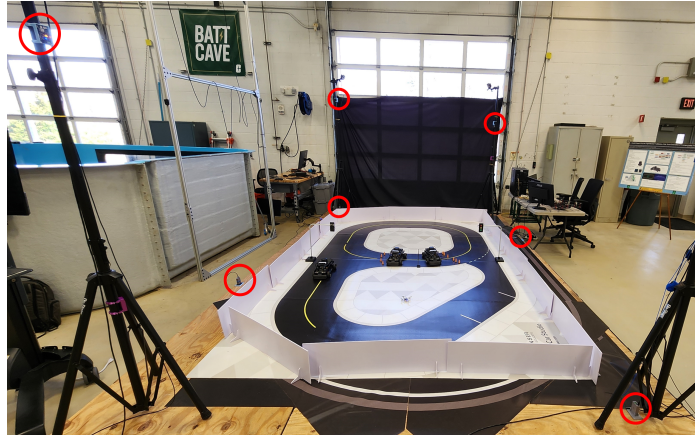


Fig. 2 Laboratory Flying Environment with Loco Positioning Nodes Circled in Red

B. Sensors

The Crazyflie 2.1 comes with a 7 DOF IMU. The onboard sensors are:

- 1) 3-axis Gyroscope (BMI088)
- 2) 3-axis Accelerometer (BMI088)
- 3) High Precision Pressure Sensor (BMP388)

The BMI088, Fig. 3, is an inertial measurement unit (IMU) from Bosch [10]. It has a digital resolution of 16-bit for both the accelerometer and gyroscope. Its data output can range from 12.5 Hz to 2 kHz. Due to the limitations of the radio communication between the Crazyflie and the Crazyradio, IMU data during this study was logged at 100 Hz. The BMP388, Fig. 4, is a small, precise, low power pressure sensor from Bosch [11]. It measures both temperature and pressure. It has a maximum sampling rate of 200 Hz; however, in this study, the barometer data was logged at 100 Hz.



Fig. 3 BMI088 IMU Sensor from Bosch



Fig. 4 BMP388 Barometer Sensor from Bosch

C. Positioning System

The capabilities of the Crazyflie drone can be expanded through the addition of decks. Decks, manufactured by Bitcraze, are expansion boards that can be mounted above and below the main PCB frame of the Crazyflie to add capabilities. While Bitcraze offers a multitude of options, the decks selected for use in this work added positioning capabilities to the Crazyflie. The Loco Position System was selected as the primary absolute positioning system, with the Z-ranger V2 deck utilized to improve the z-position accuracy.

The Loco Positioning System (LPS) can operate in one of two ways, two-way ranging (TWR) or time delay of arrival (TDoA). TWR is a more robust form of determining location; however, it only supports a single Crazyflie. The LPS consists of eight anchors or nodes and a loco positioning deck (tag) on each Crazyflie. The LPS relies on Ultra Wide Band radio to determine the 3D position of the Crazyflie. The anchors are positioned in the flying environment and their positions are measured to form the reference, as pictured in Fig. 2. The LPS can reach positional accuracies of ± 10 cm from the actual position of each vehicle [12].

One node was placed in each corner of the cubic flying environment. The absolute positions of the nodes could not be measured with sufficient accuracy due to the uncertainty of the mounting locations; therefore, the measured coordinates were approximate. To optimize the position estimates for each node, pairwise distances between all nodes were measured using a laser. A MATLAB script was used to optimize the originally measured positions to fit the distance matrix. This was done through constrained nonlinear optimization using MATLAB's 'fmincon' function. The maximum difference between the original positions and the distance matrix was reduced from 24 cm to 3 cm.

Preliminary test flights with the Crazyflie drones revealed that the LPS performed to its listed accuracy in the x-y plane; however, there were variations of much greater than ± 10 cm in the z direction. To improve the accuracy of the z-position, the Z-Ranger V2 deck was implemented. The z-ranger deck, Fig. 5, utilizes a VL53L1x ToF sensor to measure distances up to 4 meters [13]. This sensor provided much greater accuracy for the z-position estimate, assisting the Crazyflie in hovering at a stable altitude.

D. Air Vortex Generator

To generate the desired air vortex ring in a laboratory setting, an air vortex cannon toy was used. Specifically, the Airzooka from Toysmith was used. The cannon consists of a plastic barrel and a loose non-elastic polythene membrane. The membrane is pulled back by the operator, allowing for the barrel to be filled with a greater volume of air. The membrane is tensioned with a bungee cord, which, upon release, forces the air out of the barrel. The sudden reduction in barrel diameter at the outlet, forces the air into a vortex ring shape. The Airzooka can be seen in Fig. 6.

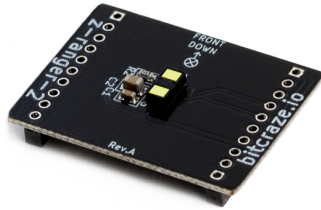


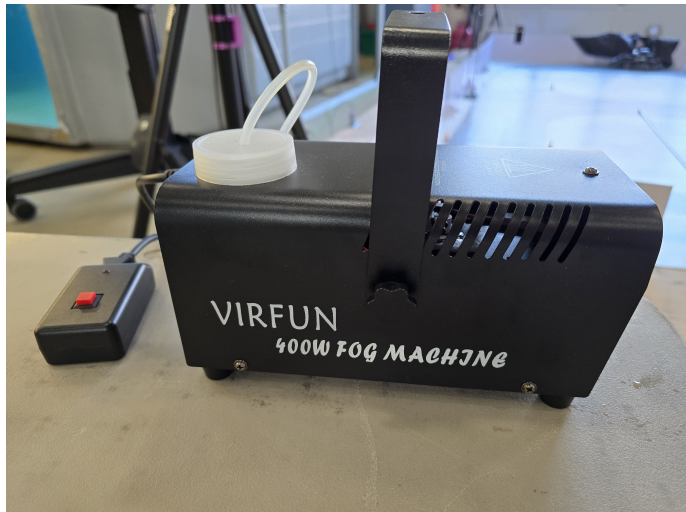
Fig. 5 Z-Ranger v2 Deck from Bitcraze



Fig. 6 Airzooka - Air Vortex Generator

E. Smoke Generator

To allow for visualization of the ring vortex generated by the Airzooka, a VIRFUN 400W fog machine was used. By filling the air vortex cannon with smoke prior to firing, the ring vortex could be easily visualized as it moved through the air. Fog Worx high density fog juice was used.



(a) VIRFUN 400W Fog Machine



(b) Fog Worx Fog Juice

Fig. 7 Smoke Generator

IV. Control Methodology

The Crazyflie Python Library contains multiple different flight commanders, including the commander, motion commander, and high level commander. The commander allows for control of the Crazyflie through a variety of command types including sending roll, pitch, yaw rate, and thrust commands; sending x, y, and z velocity commands; and sending absolute position setpoints. The motion commander allows for relative motion commands including forward, left, right, back, up, and down. The high level commander was used in this work due to previous experience and success with this commander.

A. High Level Commander

The high level commander is used for sending high level setpoints to the Crazyflie [14]. It includes commands such as takeoff, land, go to, and start trajectory. For the purposes of this study, the flight path for the Crazyflie only involved

taking off, hovering, and landing. To achieve this, the high level commands of takeoff, go to, and land were used. The takeoff function requires two inputs: a height to takeoff to and a time to get there. The land function requires similar inputs: a height to land at and a time to get there. The go to function requires five inputs: x, y, z, yaw, and duration. The duration value defines the time it should take the Crazyflie to reach the position. The go to function causes the Crazyflie to transition smoothly from its current state to the target position. It creates a flight trajectory that ends at the goal with zero velocity and acceleration. In addition, the jerk is constrained to zero at both the starting and ending points. By repeatedly commanding the same position using the go to function, a hover flight was achieved.

V. Experimental Design

To investigate the effects of impulsive aerodynamic disturbances on a micro-aerial vehicle, a series of controlled experiments were conducted using the Crazyflie 2.1 quadrotor. The objective of these trials was to analyze the UAV's response to directed vortex ring disturbances generated by an air vortex cannon while in hovering flight.

A. Test Setup and Initialization

The experiments were conducted in a controlled indoor flight environment to minimize external environmental influences. The Crazyflie 2.1 was placed at the center of the flight area on the ground, oriented such that its yaw angle was aligned in the positive x-direction. A Python script was used to automate the takeoff, hovering, landing, and data collection procedure. The script executed the following steps:

- 1) **Position Estimator Reset:** The onboard position estimator was reset to ensure accurate localization.
- 2) **Kalman Filter Convergence:** The system was given time to allow the onboard Kalman filter to stabilize before initiating flight commands.
- 3) **Takeoff Maneuver:** The drone was commanded to take off to a specified altitude of 1 meter using the high-level commander's "takeoff" function.
- 4) **Hovering Phase:** The quadrotor maintained a stationary hover for 15 seconds during which the external disturbances were introduced, using the high-level commander's "go_to" function.
- 5) **Landing Maneuver:** The drone was commanded to land at an altitude of 0 meters using the high-level commander's "land" function.

B. Vortex Cannon Disturbance

During the 15 second hovering phase, an air vortex cannon was manually fired at the drone to introduce an impulsive aerodynamic disturbance. The vortex blasts were generated at varying distances from the quadrotor to evaluate the intensity-dependent effects of the disturbance. The firing distances ranged from 3 feet to 14 feet, allowing for a systematic analysis of UAV stability under different impulse magnitudes.

To enhance visualization of the vortex interaction, trials were divided into two groups:

- 25 trials with smoke-filled vortex rings, which improved visibility of the vortex flow in the video analysis.
- 25 trials without smoke, ensuring that the presence of smoke did not introduce additional aerodynamic effects.

C. Data Collection and Recording

During each trial, the Crazyflie's onboard inertial measurement unit recorded real-time sensor data, including:

- Gyroscope (3-axis angular velocity)
- Accelerometer (3-axis linear acceleration)
- Barometer (temperature and pressure reading)

Additionally, slow-motion video recordings were captured to visually analyze the drone's response to vortex impact. A total of 50 trials were conducted to ensure statistical reliability and to observe trends in UAV response under different vortex conditions.

VI. Results

This section presents the measured and observed response of the UAV to impulsive aerodynamic disturbances from the vortex cannon. The primary focus is on the barometric pressure changes recorded by the onboard barometer, as well as the UAV's ability to maintain stable flight following impact.

A. Barometric Pressure Response

To quantify the magnitude of the aerodynamic disturbance, the barometer data was analyzed to determine the maximum change in pressure (ΔP) between consecutive measurements. A MATLAB script was used to compute the maximum ΔP for each trial, and these values were averaged across different experimental conditions. The result from each trial was categorized into three groups based on the UAV's response:

- 1) **Missed Target:** Trials where the vortex ring did not directly impact the UAV.
- 2) **Recovered Flight:** Trials where the vortex ring hit the UAV, but it was able to stabilize and maintain flight.
- 3) **Unrecoverable Flight:** Trials where the vortex ring hit the UAV, causing destabilization and an unrecoverable crash.

The summary of these results is presented in Table 1, showing the relationship between ΔP and UAV stability.

Table 1 Summary of Maximum ΔP Measurements

Result	Average ΔP	Std ΔP	n
Miss	0.087	0.096	7
Hit	0.184	0.111	33
Disabled	0.206	0.139	10

These results indicate a clear correlation between the magnitude of the pressure disturbance and the UAV's ability to recover. The pressure fluctuations were significantly higher in cases where the UAV lost stability, suggesting that the change in pressure is largely responsible for the destabilization of the UAV.

B. Case Study: Side-by-Side Comparison of Trials 04 and 05

To further investigate the impact of vortex disturbances, a detailed comparison was performed on two trials with nearly identical conditions. In Trial 04 and Trial 05, the vortex cannon was positioned 10 feet from the target, both shots were direct hits, and the vortex rings were smoke-filled to enhance visualization. Despite these similarities, the UAV successfully recovered in Trial 04, while in Trial 05, it destabilized and crashed.

The difference in responses as measured by the IMU data can be seen in side-by-side comparisons in Figures 8 through 15. In the pressure measurements, it can be seen that both trials experienced a drop in the range of 0.2 mbar (20 pascals). In fact, Trial 04 experienced a maximum ΔP of 0.2475mbar/0.01seconds, compared to the maximum ΔP of 0.21631mbar/0.01seconds of Trial 05. This shows that while the magnitude of the pressure difference is important, it is not the most significant factor in determining the UAV's ability to recover. The next set of data points analyzed was the linear acceleration. When the vortex ring initially impacts the UAV, it propels the UAV in the +x direction, as shown by the spike in the x acceleration data. In Trial 04, around the 800th data point, the vortex ring impacted the UAV, propelling it forward at a maximum rate of 0.78 Gs. In Trial 05, the vortex ring first makes impact just before the 1000th data point. It created a very comparable x-acceleration of 0.76 Gs. This shows that the relationship between the forces generated on the UAV and the UAV's ability to recover are very complex and there are several other factors that contribute. Figures 16 and 17 show the still images of the flight for both trials. In Trial 04, after the vortex ring makes contact, the UAV moves in the +x direction in frame 2, but maintains relatively level pitch and roll angles. The pitch and roll angles do not exceed 10 degrees during this flight. In frame 3, it can be seen that the UAV moves back to its original position. It then loses a bit of altitude in frame 4, before fully recovering by frame 5. Although the experimental conditions were identical, the images of Trial 05 show a very different story. In frame 2, it can be seen that the vortex ring propels the UAV in the +x direction at a very similar rate to that of Trial 04. The difference in Trial 05 is the state angles at which the UAV experiences. While the pitch and roll did not exceed 10 degrees for Trial 04, the initial roll experienced by the UAV in Trial 05 exceeded 27 degrees, while the initial pitch exceeded -23 degrees. Frame 3 illustrates how the UAV experienced a much more challenging state to recover from. In frame 4, the UAV is attempting to return to its nominal state; however, it can be seen in the following frame, that the UAV over-corrected and will crash very shortly.

The side-by-side comparison between two very similar trials, with drastically different outcomes illustrates how sensitive a UAV's control system can be to sudden forces. The comparison shows how the UAV's ability to recover is not directly related to the magnitude of the force alone, but rather to the maximum displacement experienced by the UAV. In the case where the drone experienced relatively small changes in state angles, it was able to recover. In the case where the UAV experienced slightly smaller forces, but greater displacements around the pitch and roll axis, the UAV was unable to recover.

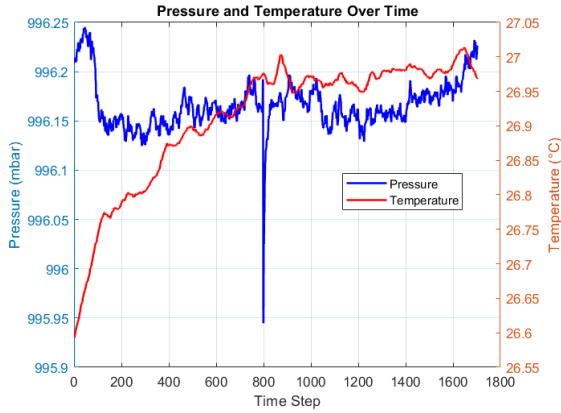


Fig. 8 Trial 04 Temperature and Pressure

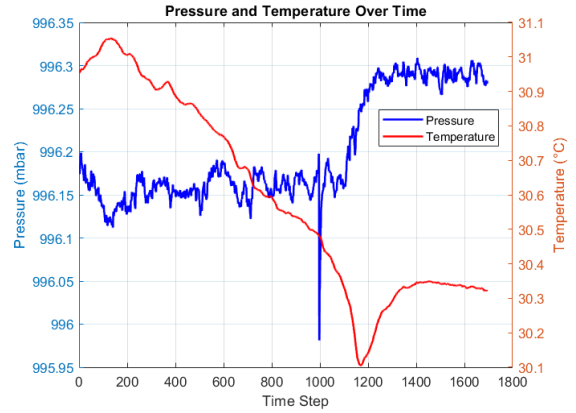


Fig. 9 Trial 05 Temperature and Pressure

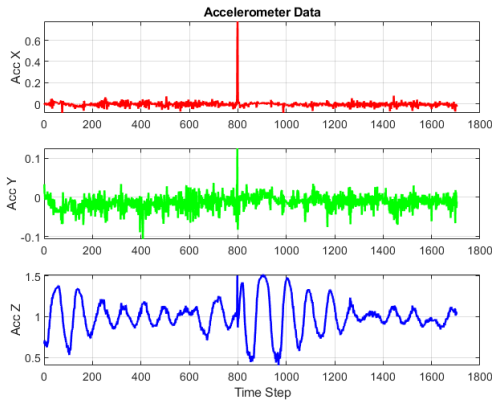


Fig. 10 Trial 04 Acceleration

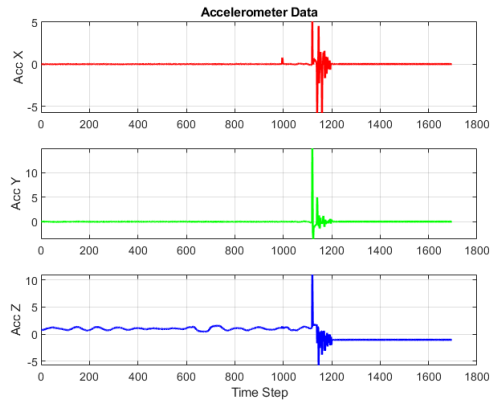


Fig. 11 Trial 05 Acceleration

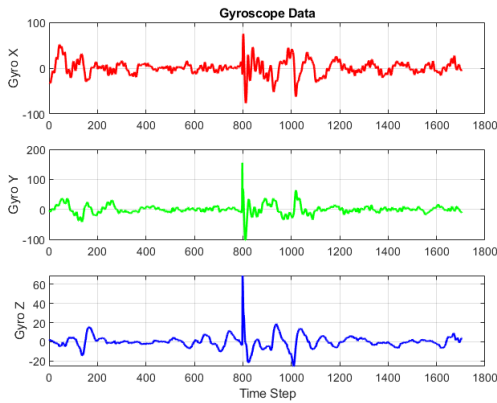


Fig. 12 Trial 04 Gyroscope

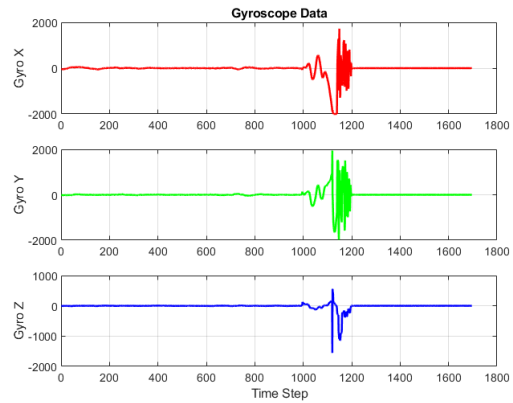


Fig. 13 Trial 05 Gyroscope

Analysis of the timing of the oscillations of the IMU data showed that the pressure drop, as measured by the barometer, always preceded any perturbations of the accelerometer or gyroscope. Not only does this indicate that it is indeed the pressure change that causes the UAV to be disturbed, but that the barometer could potentially be used as an early warning system. The pressure drop precedes the perturbations by approximately 0.1 to 0.2 seconds. If the UAV is able to recognize this pressure drop, there is a potential for the execution of a preemptive maneuver that could help

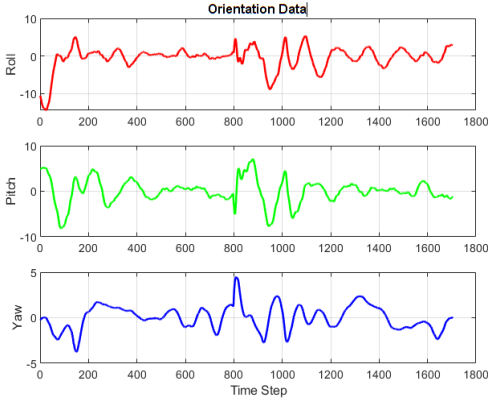


Fig. 14 Trial 04 Orientation

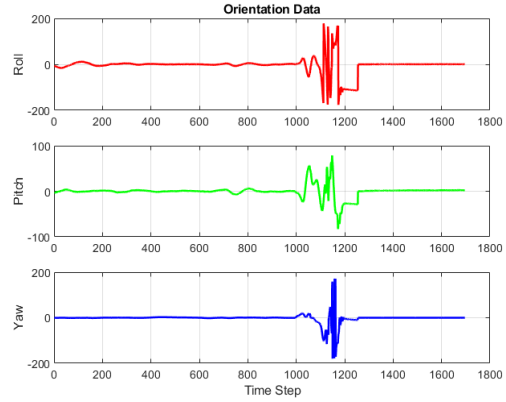


Fig. 15 Trial 05 Orientation

stabilize the drone. For example, if the vortex ring causes the UAV to rotate to an undesirable negative pitch angle, the UAV could attempt to rotate to the corresponding positive pitch angle once the pressure drop is experienced. Therefore, when the vortex ring forces the rotation, the preemptive maneuver will cancel out the effect, leading to stable flight. Table 2 shows how the initial maximum pitch and roll angles for the flights in which the UAV was unable to recover far exceeded those of flights in which the UAV successfully recovered.

Table 2 Summary of Pitch and Roll Angles for Recovered versus Crashed

Result	Average Max Pitch	Std	Average Max Roll	Std
Recovered	13.4	13.9	22.5	39.4
Disabled	32	10.5	81.9	82.0

In addition to the above results, interesting behaviors were noticed in certain trials in which the operator missed the target. In cases in which the vortex passed directly over the UAV, the UAV typically responded with a sudden increase in altitude followed by a rapid decent and stabilization. This indicates that the passing vortex created an area of lower pressure above the UAV, pulling the UAV up into its wake. Then, the UAV over-corrected, reducing its thrust too much, causing it to drop below the hover height, before stabilizing.

VII. Conclusion

The goal of this work was to characterize a UAV's response to sudden aerodynamic forces. Using the Crazyflie 2.1 drone and an air vortex cannon, fifty trials were carried out. During each trial, the onboard IMU data was logged and slow-motion video was captured. Analysis of these results showed that as the distance between the UAV and the air vortex cannon decreases, the pressure differential experienced by the UAV increases. Greater pressure differential was generally associated with a higher likelihood of destabilization and loss of control. However, the ability of the UAV to recover was found to depend on more than just the magnitude of the pressure differential. By comparing trials under identical conditions but with different outcomes, it was determined that recovery success is primarily influenced by the maximum initial displacements around the pitch and roll axes caused by the vortex ring. In cases where the UAV failed to recover, the induced pitch angle was more than twice as large, and the roll angle more than three times as large, compared to cases where stable flight was maintained. Future work may include developing preemptive maneuvers that the UAV can use to mitigate the effects of sudden aerodynamic disturbances. This could involve real-time adjustments to pitch and roll based on onboard sensor feedback, improving the UAV's ability to maintain stability after impact.

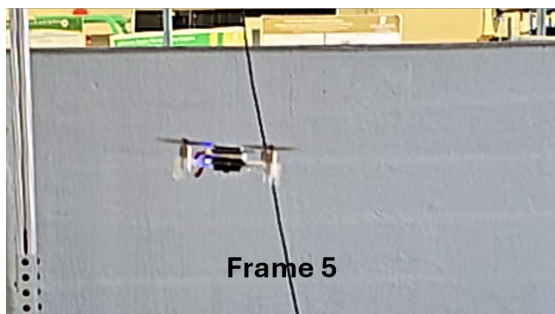
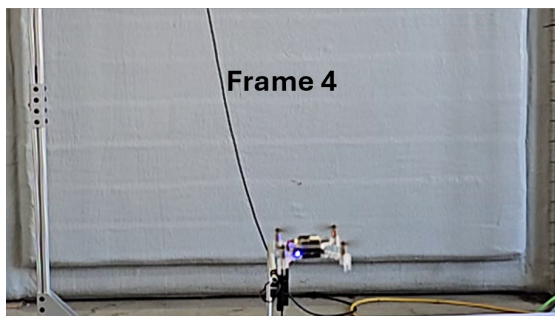
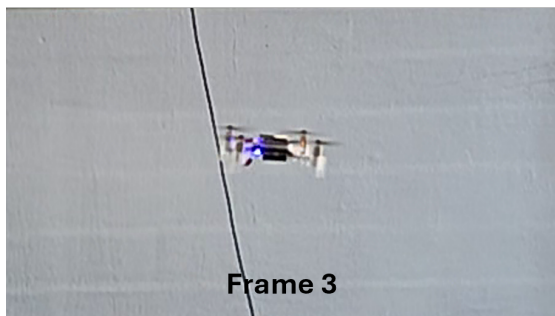
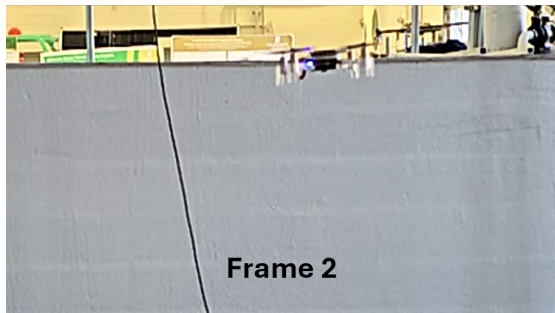
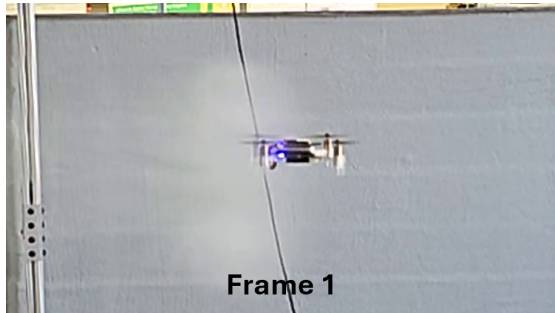


Fig. 16 Trial 04 Video Captures

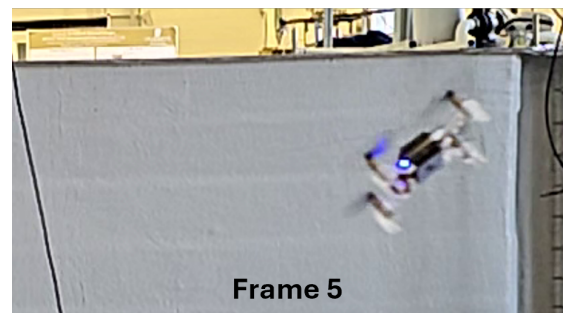
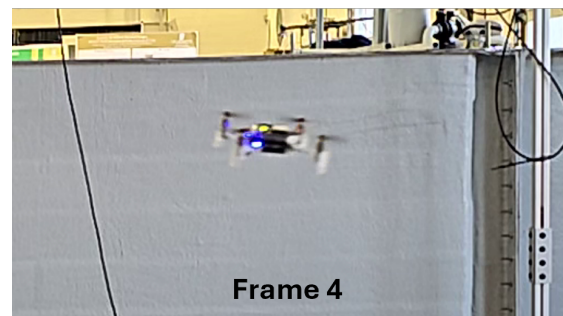
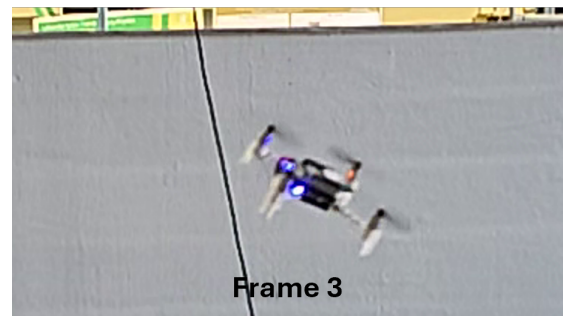
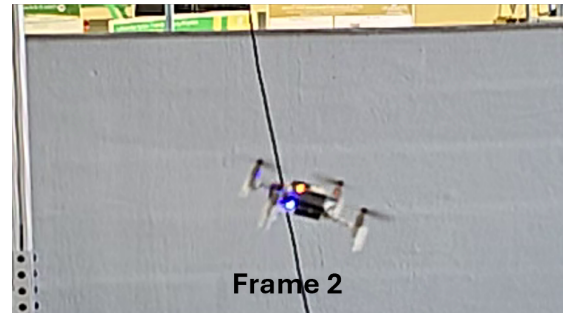
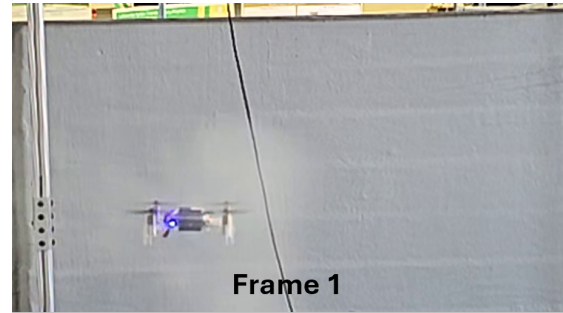


Fig. 17 Trial 05 Video Captures

Funding Sources

This work was supported by the University of North Carolina at Charlotte's Office of Undergraduate Research (OUR) and by NSF grant No. 2301475.

Acknowledgments

The author thanks Dr. Artur Wolek and Nick Kakavitsas for providing guidance throughout this research and for paper review. The author also thanks Dr. Amir Ghasemi for allowing access to the smart city environment which was used throughout testing.

References

- [1] Martin, J. E., Saul, V., Novick, D., and Allen, D., "Assessing the Vulnerability of Unmanned Aircraft Systems to Directed Acoustic Energy," Tech. rep., Sandia National Laboratories, 2020.
- [2] Feng, X., Yang, Z., and Nie, Y., "Investigation of the Overall Damage Assessment Method Used for Unmanned Aerial Vehicles Subjected to Blast Waves," *Aerospace*, Vol. 11, No. 8, 2024. <https://doi.org/10.3390/aerospace11080651>, URL <https://www.mdpi.com/2226-4310/11/8/651>.
- [3] Grzywiński, S., and Żygadło, S., "Research of Vibroacoustic Interference Occuring on UAV," *Engineering Mechanics 2019*, 2019. URL <https://api.semanticscholar.org/CorpusID:242345969>.
- [4] Gupta, D., Sane, S. P., and Arakeri, J. H., "Design and development of a vortex ring generator to study the impact of the ring as a gust," *bioRxiv*, 2020. <https://doi.org/10.1101/2020.10.12.331777>, URL <https://www.biorxiv.org/content/early/2020/10/12/2020.10.12.331777>.
- [5] Zieg, P., and Liu, Y., *An Experimental Study on the Impact of Blast Wave on UAV Aerodynamic Properties*, AIAA, 2021. <https://doi.org/10.2514/6.2022-0350>, URL <https://arc.aiaa.org/doi/abs/10.2514/6.2022-0350>.
- [6] Tao, Y., and Zhang, S., "Research on the Vibration and Wave Propagation in Ship-Borne Tethered UAV Using Stress Wave Method," *Drones*, Vol. 6, No. 11, 2022. <https://doi.org/10.3390/drones6110349>, URL <https://www.mdpi.com/2504-446X/6/11/349>.
- [7] BitCrazeAB, "Crazyflie 2.1," <https://www.bitcraze.io/products/crazyflie-2-1/>, 2023.
- [8] BitCrazeAB, "Crazyradio 2.0," <https://www.bitcraze.io/products/crazyradio-2-0/>, 2023.
- [9] BitCrazeAB, "Crazyflie Python Library," <https://github.com/bitcraze/crazyflie-lib-python>, 2023.
- [10] Bosch, "Inertial Measurement Unit: BMI088," <https://www.bosch-sensortec.com/products/motion-sensors/imus/bmi088/>, 2024.
- [11] Bosch, "Pressure sensor BMP388," <https://www.bosch-sensortec.com/products/environmental-sensors/pressure-sensors/bmp388/>, 2024.
- [12] BitCrazeAB, "Loco Positioning system," <https://www.bitcraze.io/documentation/system/positioning/loco-positioning-system/>, 2023.
- [13] BitCrazeAB, "Z-ranger deck v2," <https://www.bitcraze.io/products/z-ranger-deck-v2/>, 2023.
- [14] BitCrazeAB, "high_level_commander.py," https://github.com/bitcraze/crazyflie-lib-python/blob/master/cflib/crazyflie/high_level_commander.py, 2021.